PERGAMON

International Journal of Solids and Structures 40 (2003) 2381–2399

INTERNATIONAL JOURNAL OF SOLIDS and STRUCTURES

www.elsevier.com/locate/ijsolstr

# A moving conducting crack at the interface of two dissimilar piezoelectric materials

X. Wang *, Z. Zhong, F.L. Wu

*Key Laboratory of Solid Mechanics of MOE, Department of Engineering Mechanics and Technology, Tongji University, Shanghai 200092, PR China*

Received 19 August 2002

**Abstract**

The problem of a Yoffe-type conducting crack moving with a constant velocity at the interface of two dissimilar piezoelectric half planes is investigated by employing complex variable method. Solutions for the complex potentials are derived. Explicit expressions for the field components on the interface are presented based on the obtained complex potentials. It is observed that the nature of the field singularities near the crack tip is intimately dependent on the crack moving velocity. In the extremely low speed regime, the singularities are $\delta = -1/2 \pm i\varepsilon_1$; in the low speed regime, the singularities are $\delta = -1 \pm i\varepsilon_2$; in the intermediate speed regime, the singularities are $\delta = -1/2 \pm k$; in the high speed regime, the singularities are $\delta = -1 \pm i\varepsilon_3$; in the extremely high speed regime, the singularities are $\delta = -1/2 \pm i\varepsilon_4$. $\varepsilon_i$ $(i = 1\text{–}4)$ and $k$ are also explicitly given. A Yoffe-type moving conducting crack in a homogeneous piezoelectric material is treated as a special case. The numerical results demonstrate that the moving velocity $V$ will exert a significant influence on the value of the singularities, and on the field component distributions along the interface.


*Keywords:* Piezoelectricity; Moving conducting crack; Singularities; Speed regime

## 1. Introduction

A Yoffe-type moving crack in piezoelectric materials has been considered by several investigators (see for example Chen and Yu, 1997, 1999; Chen et al., 1998; Li et al., 2000; Kwon et al., 2000; Li and Weng, 2002) to probe the effect of crack moving velocity on the electromechanical coupling response of smart systems made of piezoelectric materials. The main results from these investigations are

- Stresses and electric displacements exhibit inverse square root singularities near the tip of a crack in a homogeneous piezoelectric material (Chen and Yu, 1997; Kwon et al., 2000), or at the piezoelectric

* Corresponding author.
*E-mail address:* wjq_wang@sina.com (X. Wang).

0020-7683/03/$ - see front matter © 2003 Elsevier Science Ltd. All rights reserved.
doi:10.1016/S0020-7683(03)00060-X

bimaterial interface (Chen et al., 1998; Li et al., 2000), or in a functionally graded piezoelectric material (Li and Weng, 2002);

- The stress and electric displacement intensity factors are independent of the crack moving velocity and material constants for a crack in a homogeneous piezoelectric plane, otherwise they will rely on the crack moving velocity and material constants.

The electrical boundary conditions on the crack surfaces in the above listed studies were assumed to be impermeable (insulating) or permeable. The conducting cracks in piezoelectric materials are also an important failure mode (Suo, 1993; Li and Mataga, 1996; Ru, 1999; Wang and Zhong, 2002), and possess some unique interesting features (Li and Mataga, 1996; Wang and Zhong, 2002). To the best of the authors' knowledge, the problem of a moving conducting crack of Yoffe-type in piezoelectric materials has not yet been resolved. Therefore, we will consider a Yoffe-type moving conducting crack at the piezoelectric bimaterial interface. The holomorphic function vectors characterizing the electroelastic fields in the bimaterials are derived. Field component distributions on the interface are presented from the obtained analytic function vectors. It is observed that the nature of the singularities is dependent on the crack moving velocity. The field components exhibit the oscillatory singularities $-1/2 \pm i\varepsilon_1$ when the crack moving velocity is within the *extremely low speed regime*. The field components exhibit the singularities $-1 \pm i\varepsilon_2$ when the crack moving velocity is within the *low speed regime*. The field components exhibit the real power type singularities $-1/2 \pm k$ when the crack moving velocity is within the *intermediate speed regime*. The field components exhibit the singularities $-1 \pm i\varepsilon_3$ when the crack moving velocity is within the *high speed regime*. The field components exhibit the oscillatory singularities $-1/2 \pm i\varepsilon_4$ when the crack moving velocity is within the *extremely high speed regime*. The real constants $\varepsilon_1$, $\varepsilon_2$, $k$, $\varepsilon_3$, $\varepsilon_4$, which are explicitly given, depend on the crack moving velocity and electroelastic constants of the bimaterials. The problem of a Yoffe-type moving conducting crack in a homogeneous piezoelectric material is considered as a special case of this research, and stress and electric field intensity factors are introduced to characterize the inverse square root singular field near the crack tips. The numerical results indicate that the crack moving velocity will exert a significant influence on the singularities, and on the field component distributions along the bimaterial interface.

## 2. Basic equations and boundary conditions

Consider a crack of fixed length $2a$ moving with a constant velocity $V$ along the interface of two dissimilar piezoelectric half planes, as shown in Fig. 1. This type of crack is the so-called Yoffe-type moving crack (Yoffe, 1951; Li and Weng, 2002). Both the upper half plane, denoted by #1, and the lower half plane, denoted by #2, are transversely isotropic with the poling direction parallel to the $x_3$-axis. Under anti-plane mechanical loading and in-plane electric loading, the governing field equations and the constitutive equations can be simplified considerably as

—governing field equations:

$$\sigma_{31,1} + \sigma_{32,2} = \rho \frac{\partial^2 w}{\partial t^2}, \quad E_{2,1} - E_{1,2} = 0 \tag{1}$$

—linear, piezoelectric constitutive equations:

$$\begin{bmatrix} \sigma_{32} \\ -E_1 \end{bmatrix} = \begin{bmatrix} c_{44} + \dfrac{e_{15}^2}{\varepsilon_{11}} & 0 \\ 0 & \dfrac{1}{\varepsilon_{11}} \end{bmatrix} \begin{bmatrix} w_{,2} \\ \varphi_{,2} \end{bmatrix} + \begin{bmatrix} 0 & -\dfrac{e_{15}}{\varepsilon_{11}} \\ \dfrac{e_{15}}{\varepsilon_{11}} & 0 \end{bmatrix} \begin{bmatrix} w_{,1} \\ \varphi_{,1} \end{bmatrix} \tag{2a}$$

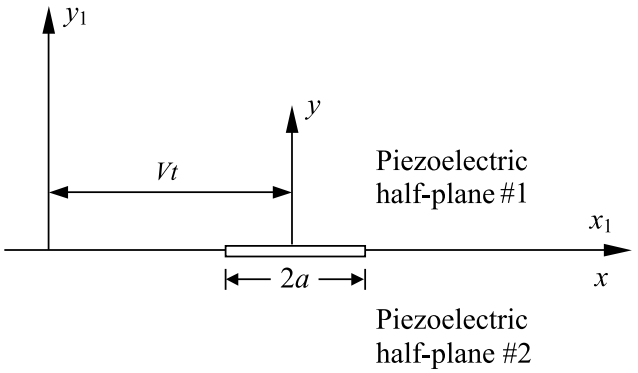


Fig. 1. A crack moving at the interface of two dissimilar piezoelectric materials.

$$\begin{bmatrix} \sigma_{31} \\ E_2 \end{bmatrix} = \begin{bmatrix} c_{44} + \dfrac{e_{15}^2}{\varepsilon_{11}} & 0 \\ 0 & \dfrac{1}{\varepsilon_{11}} \end{bmatrix} \begin{bmatrix} w_{,1} \\ \varphi_{,1} \end{bmatrix} - \begin{bmatrix} 0 & -\dfrac{e_{15}}{\varepsilon_{11}} \\ \dfrac{e_{15}}{\varepsilon_{11}} & 0 \end{bmatrix} \begin{bmatrix} w_{,2} \\ \varphi_{,2} \end{bmatrix} \tag{2b}$$

where $c_{44}$, $e_{15}$, $\varepsilon_{11}$ are the elastic stiffness, the piezoelectric constant and the dielectric permittivity, respectively, $\sigma_{31}$, $\sigma_{32}$ are the stress components, $E_1$, $E_2$ are the electric field components, $\rho$ is the mass density, $w$ is out of plane displacement, and the function $\varphi$ is defined in terms of the electric displacements as follows:

$$D_2 = \varphi_{,1}, \quad D_1 = -\varphi_{,2} \tag{3}$$

Substitution of Eqs. (2a) and (2b) into (1) will yield the following canonical form:

$$\begin{aligned} \nabla^2 w &= \frac{1}{s^2} \frac{\partial^2 w}{\partial t^2} \\ \nabla^2 \varphi &= 0 \end{aligned} \tag{4}$$

where $\nabla^2 = (\partial^2/\partial x_1^2) + (\partial^2/\partial x_2^2)$ is the two-dimensional Laplacian operator, and $s$ is the speed of the piezoelectrically stiffened bulk shear wave given by

$$s = \sqrt{\frac{\bar{c}_{44}}{\rho}} \tag{5}$$

where $\bar{c}_{44} = c_{44} + e_{15}^2/\varepsilon_{11}$ is the piezoelectrically stiffened elastic constant.

Since the discussed problem is in a steady state, the Galilean transformation can be conveniently introduced as follows:

$$x = x_1 - Vt, \quad y = x_2, \quad z = x_3 \tag{6}$$

Then (4) can be cast into the form:

$$\beta^2 \frac{\partial^2 w}{\partial x^2} + \frac{\partial^2 w}{\partial y^2} = 0, \quad \frac{\partial^2 \varphi}{\partial x^2} + \frac{\partial^2 \varphi}{\partial y^2} = 0 \tag{7}$$

where

$$\beta = \sqrt{1 - V^2/s^2} \tag{8}$$

The general solutions to (7) are

$$\mathbf{U} = \begin{bmatrix} w \\ \varphi \end{bmatrix} = \mathrm{Im}\{\mathbf{f}(z)\} \tag{9}$$

where $\mathbf{f}(z) = [\, f_1(z_1) \quad f_2(z) \,]^{\mathrm{T}}$, and $z_1 = x + \mathrm{i}\beta y$, $z = x + \mathrm{i}y$.

The stresses and electric fields can be expressed in terms of $\mathbf{f}(z)$ as follows:

$$\begin{bmatrix} \sigma_{32} \\ -E_1 \end{bmatrix} = \mathrm{Re}\left\{ \begin{bmatrix} \beta \bar{c}_{44} & \mathrm{i}\dfrac{e_{15}}{\varepsilon_{11}} \\ -\mathrm{i}\dfrac{e_{15}}{\varepsilon_{11}} & \dfrac{1}{\varepsilon_{11}} \end{bmatrix} \mathbf{f}'(z) \right\} = \mathrm{Re}\{\mathbf{C}\mathbf{f}'(z)\} \tag{10a}$$

$$\begin{bmatrix} \sigma_{31} \\ E_2 \end{bmatrix} = \mathrm{Im}\left\{ \begin{bmatrix} \bar{c}_{44} & \mathrm{i}\dfrac{e_{15}}{\varepsilon_{11}} \\ -\mathrm{i}\beta\dfrac{e_{15}}{\varepsilon_{11}} & \dfrac{1}{\varepsilon_{11}} \end{bmatrix} \mathbf{f}'(z) \right\} \tag{10b}$$

Due to the linear property, the principle of superposition can be used here and the solution can be represented as the sum of a uniform electroelastic field in the uncracked piezoelectric bimaterials and the disturbance field caused by the moving conducting crack. The boundary and continuity conditions for this disturbance problem are

$$\sigma_{32}^{(1)}(x, 0^+) = \sigma_{32}^{(2)}(x, 0^-) = -\sigma_{32}^{\infty}, \quad |x| < a \tag{11}$$

$$E_1^{(1)}(x, 0^+) = E_1^{(2)}(x, 0^-) = -E_1^{\infty}, \quad |x| < a \tag{12}$$

$$\sigma_{32}^{(1)}(x, 0^+) = \sigma_{32}^{(2)}(x, 0^-), \quad |x| \geqslant a \tag{13}$$

$$\gamma_{31}^{(1)}(x, 0^+) = \gamma_{31}^{(2)}(x, 0^-), \quad |x| \geqslant a \tag{14}$$

$$E_1^{(1)}(x, 0^+) = E_1^{(2)}(x, 0^-), \quad |x| \geqslant a \tag{15}$$

$$D_2^{(1)}(x, 0^+) = D_2^{(2)}(x, 0^-), \quad |x| \geqslant a \tag{16}$$

$$\begin{matrix} \sigma_{3i}^{(1)} = \sigma_{3i}^{(2)} = 0, \\ D_i^{(1)} = D_i^{(2)} = 0. \end{matrix} \quad (i = 1, 2) \quad |x + \mathrm{i}y| \to \infty \tag{17}$$

where the superscripts "(1)" and "(2)" denote the physical quantities pertaining to the upper half plane and the lower half plane, respectively. In the following analysis, the quantities in the upper half plane #1 and the lower half plane #2 will be identified by the subscripts 1 and 2, respectively. When analyzing this boundary value problem, it is more convenient to replace $z_1$ by $z$. When calculating electroelastic field from (9) and (10a) and (10b), it is needed to reinterpret $z$ by $z_1$ accordingly.

## 3. Exact solution

The continuity conditions of tractions and tangential electric field across the total real axis can be expressed as

$$\mathbf{C}_1\mathbf{f}_1'^{+}(x) + \overline{\mathbf{C}_1}\,\bar{\mathbf{f}}_1'^{-}(x) = \mathbf{C}_2\mathbf{f}_2'^{-}(x) + \overline{\mathbf{C}_2}\,\bar{\mathbf{f}}_2'^{+}(x), \quad -\infty < x < +\infty \tag{18}$$

It follows from the above condition that

$$\bar{\mathbf{f}}_2'(z) = \overline{\mathbf{C}_2^{-1}}\mathbf{C}_1\mathbf{f}_1'(z), \quad \bar{\mathbf{f}}_1'(z) = \overline{\mathbf{C}_1^{-1}}\mathbf{C}_2\mathbf{f}_2'(z) \tag{19}$$

Meanwhile, the continuity conditions of out of plane displacement and normal electric displacement on the bonded part of the interface (14) and (16) can be expressed as

$$\mathbf{f}_1'^{+}(x) - \bar{\mathbf{f}}_1'^{-}(x) = \mathbf{f}_2'^{-}(x) - \bar{\mathbf{f}}_2'^{+}(x), \quad |x| \geqslant a \tag{20}$$

Inserting the relationships (19) into (20) will result in

$$\left(\mathbf{C}_1^{-1} + \overline{\mathbf{C}_2^{-1}}\right)\mathbf{C}_1\mathbf{f}_1'^{+}(x) = \left(\overline{\mathbf{C}_1^{-1}} + \mathbf{C}_2^{-1}\right)\mathbf{C}_2\mathbf{f}_2'^{-}(x), \quad |x| \geqslant a \tag{21}$$

In view of the above relationship, we can introduce an auxiliary function vector $\mathbf{h}(z)$ defined by

$$\mathbf{h}(z) = \begin{cases} \mathbf{M}\mathbf{C}_1\mathbf{f}_1'(z), & y > 0 \\ \overline{\mathbf{M}}\mathbf{C}_2\mathbf{f}_2'(z), & y < 0 \end{cases} \tag{22}$$

where the $2 \times 2$ Hermitian matrix $\mathbf{M}$ is given by

$$\mathbf{M} = \begin{bmatrix} M_{11} & \mathrm{i}M_{12} \\ -\mathrm{i}M_{12} & M_{22} \end{bmatrix} = \mathbf{C}_1^{-1} + \overline{\mathbf{C}_2^{-1}} \tag{23}$$

with the three real constants $M_{11}$, $M_{22}$ and $M_{12}$ given by

$$\begin{aligned} M_{11} &= \frac{1}{\bar{c}_{44}^{(1)}}\frac{1}{\beta^{(1)} - (k_e^{(1)})^2} + \frac{1}{\bar{c}_{44}^{(2)}}\frac{1}{\beta^{(2)} - (k_e^{(2)})^2} \\ M_{22} &= \frac{\beta^{(1)}\varepsilon_{11}^{(1)}}{\beta^{(1)} - (k_e^{(1)})^2} + \frac{\beta^{(2)}\varepsilon_{11}^{(2)}}{\beta^{(2)} - (k_e^{(2)})^2} \\ M_{12} &= \frac{e_{15}^{(2)}}{\bar{c}_{44}^{(2)}}\frac{1}{\beta^{(2)} - (k_e^{(2)})^2} - \frac{e_{15}^{(1)}}{\bar{c}_{44}^{(1)}}\frac{1}{\beta^{(1)} - (k_e^{(1)})^2} \end{aligned} \tag{24}$$

where $k_e^{(i)} = \sqrt{(e_{15}^{(i)})^2/(\bar{c}_{44}^{(i)}\varepsilon_{11}^{(i)})}$, $(i = 1, 2)$ are the electromechanical coupling factors.

The traction and tangential electric displacement conditions on the crack surfaces (11) and (12) can be expressed in terms of the above newly introduced function vector $\mathbf{h}(z)$ as

$$\mathbf{M}^{-1}\mathbf{h}^{+}(x) + \overline{\mathbf{M}}^{-1}\mathbf{h}^{-}(x) = 2\mathbf{T}, \quad |x| < a \tag{25}$$

where

$$\mathbf{T} = \begin{bmatrix} -\sigma_{32}^{\infty} \\ E_1^{\infty} \end{bmatrix} \tag{26}$$

In order to solve the above Riemann–Hilbert problem of vector form, we consider the following eigenvalue problem:

$$(\overline{\mathbf{M}}^{-1} + e^{2\pi\mathrm{i}\delta}\mathbf{M}^{-1})\mathbf{v} = \mathbf{0} \tag{27}$$

The nature of $\delta$ will depend on the crack moving velocity $V$, which can be classified into the following five speed regimes:

- Extremely low speed regime
  The crack moving velocity in this regime satisfies the following restriction:

$$0 \leqslant V \leqslant \min\left\{c_{\mathrm{bg}}^{(1)}, c_{\mathrm{bg}}^{(2)}\right\} \tag{28}$$

where $c_{\mathrm{bg}}^{(i)} = s^{(i)}\sqrt{1-(k_e^{(i)})^4}$ $(i=1,2)$ are the Bleustein–Gulyaev wave speeds (Bleustein, 1968; Gulyaev, 1969) of the two phases.

- Low speed regime
  The crack moving velocity in this regime satisfies the following restriction:

$$\min\left\{c_{\mathrm{bg}}^{(1)}, c_{\mathrm{bg}}^{(2)}\right\} < V \leqslant \min\{V_1, V_2\} \tag{29}$$

where $V_1$ is determined by the following equation:

$$V_1 = s^{(1)}\sqrt{1-\frac{(k_e^{(1)})^4}{\chi^2}\left(\frac{\varepsilon_{11}^{(2)}}{\varepsilon_{11}^{(1)}+\varepsilon_{11}^{(2)}}\right)^2} \tag{30}$$

where $\chi$ $(0<\chi<1)$ is the real root of the following quadratic algebraic equation:

$$\chi^4 - 2\chi^3 + (1+\eta_1-\eta_2)\chi^2 - 2\eta_1\chi + \eta_1 = 0 \tag{31}$$

with

$$\eta_1 = \frac{(k_e^{(1)})^4 (s^{(1)})^2}{(s^{(2)})^2-(s^{(1)})^2}\left(\frac{\varepsilon_{11}^{(2)}}{\varepsilon_{11}^{(1)}+\varepsilon_{11}^{(2)}}\right)^2, \quad \eta_2 = \frac{(k_e^{(2)})^4 (s^{(2)})^2}{(s^{(2)})^2-(s^{(1)})^2}\left(\frac{\varepsilon_{11}^{(1)}}{\varepsilon_{11}^{(1)}+\varepsilon_{11}^{(2)}}\right)^2 \tag{32}$$

and $V_2$ is determined by the following equation:

$$V_2 = (s^{(1)})\sqrt{1-\gamma^2\left[(k_e^{(1)})^2 + \frac{\bar{c}_{44}^{(2)}}{\bar{c}_{44}^{(1)}}(k_e^{(2)})^2\right]^2} \tag{33}$$

where $\gamma$ $(0<\gamma<1)$ is the real root of the following quadratic algebraic equation:

$$\left[\left(\frac{s^{(1)}}{\bar{c}_{44}^{(1)}}\right)^2 - \left(\frac{s^{(2)}}{\bar{c}_{44}^{(2)}}\right)^2\right]\gamma^2 + 2\left(\frac{s^{(2)}}{\bar{c}_{44}^{(2)}}\right)^2\gamma - \left[\frac{(s^{(1)})^2-(s^{(2)})^2}{\left[\bar{c}_{44}^{(1)}(k_e^{(1)})^2 + \bar{c}_{44}^{(2)}(k_e^{(2)})^2\right]^2} + \left(\frac{s^{(2)}}{\bar{c}_{44}^{(2)}}\right)^2\right] = 0 \tag{34}$$

If there is no root of (34), which satisfies $0<\gamma<1$, then

$$V_2 = \min\left\{s^{(1)}, s^{(2)}\right\} \tag{35}$$

- Intermediate speed regime
  The crack moving velocity in this regime satisfies the following restriction:

$$\min\{V_1, V_2\} < V \leqslant \max\{V_1, V_2\} \tag{36}$$

- High speed regime
  The crack moving velocity in this regime satisfies the following restriction:

$$\max\{V_1, V_2\} < V \leqslant \min\left\{\max\left\{c_{\mathrm{bg}}^{(1)}, c_{\mathrm{bg}}^{(2)}\right\}, \min\left\{s^{(1)}, s^{(2)}\right\}\right\} \tag{37}$$

- Extremely high speed regime
  The crack moving velocity in this regime satisfies the following restriction:

$$\min\left\{\max\left\{c_{\mathrm{bg}}^{(1)}, c_{\mathrm{bg}}^{(2)}\right\}, \min\left\{s^{(1)}, s^{(2)}\right\}\right\} < V \leqslant \min\left\{s^{(1)}, s^{(2)}\right\} \tag{38}$$

In the following, the five speed regimes will be discussed one by one.

### 3.1. Extremely low speed regime

It can be easily checked that the following conditions hold for the components of $\mathbf{M}$:

$$M_{11} > 0, \quad M_{22} > 0, \quad M_{11}M_{22} > M_{12}^2 \tag{39}$$

Then $\delta$ in (27) can be explicitly determined to be

$$\delta = -\tfrac{1}{2} \pm \mathrm{i}\varepsilon_1 \tag{40}$$

where

$$\varepsilon_1 = \frac{1}{2\pi}\ln\frac{1+\lambda_1}{1-\lambda_1}, \quad \lambda_1 = \frac{M_{12}}{\sqrt{M_{11}M_{22}}} \quad (|\lambda_1| < 1) \tag{41}$$

The necessary and sufficient condition for the absence of oscillatory index $\varepsilon_1$ is

$$\beta^{(2)}\frac{c_{44}^{(2)}}{e_{15}^{(2)}} + (1-\beta^{(2)})\frac{e_{15}^{(2)}}{\varepsilon_{11}^{(2)}} = \beta^{(1)}\frac{c_{44}^{(1)}}{e_{15}^{(1)}} + (1-\beta^{(1)})\frac{e_{15}^{(1)}}{\varepsilon_{11}^{(1)}} \tag{42}$$

It is observed that the above condition is dependent on the crack velocity, the elastic constants, the piezoelectric constants, and the dielectric constants of the bimaterials. When $V = 0$, i.e., $\beta^{(1)} = \beta^{(2)} = 1$, expression (42) will reduce to the condition for a static interface conducting crack (Wang and Zhong, 2002). It is also apparent that when $V = \min\{c_{\mathrm{bg}}^{(1)}, c_{\mathrm{bg}}^{(2)}\}$, the upper limit of this speed regime, $\varepsilon_1$ will get to infinity.

The eigenvector $\mathbf{v}$ associated with $\delta = -\frac{1}{2} + \mathrm{i}\varepsilon_1$ is

$$\mathbf{v} = \begin{bmatrix} \sqrt{M_{11}} \\ \mathrm{i}\sqrt{M_{22}} \end{bmatrix} \tag{43}$$

Now we introduce the following coordinate transformation:

$$\mathbf{h}(z) = \mathbf{P}_1\hat{\mathbf{h}}(z), \quad \widehat{\mathbf{T}}_1 = \Delta_1\overline{\mathbf{P}}_1^{\mathrm{T}}\mathbf{T} \tag{44}$$

where

$$\mathbf{P}_1 = \begin{bmatrix} \sqrt{M_{11}} & \sqrt{M_{11}} \\ \mathrm{i}\sqrt{M_{22}} & -\mathrm{i}\sqrt{M_{22}} \end{bmatrix}, \quad \Delta_1 = \begin{bmatrix} 1-\lambda_1 & 0 \\ 0 & 1+\lambda_1 \end{bmatrix} \tag{45}$$

Then (25) can be decoupled in the new coordinate system as

$$\hat{\mathbf{h}}^{+}(x) + \Lambda_1\hat{\mathbf{h}}^{-}(x) = \widehat{\mathbf{T}}_1, \quad |x| < a \tag{46}$$

where

$$\Lambda_1 = \begin{bmatrix} e^{-2\pi\varepsilon_1} & 0 \\ 0 & e^{2\pi\varepsilon_1} \end{bmatrix} \tag{47}$$

Consequently, the explicit expression of $\mathbf{h}(z)$ can be obtained as

$$\mathbf{h}(z) = \mathbf{P}_1\left[\mathbf{I} - X_1(z)\begin{bmatrix} z+2\mathrm{i}a\varepsilon_1 & 0 \\ 0 & z-2\mathrm{i}a\varepsilon_1 \end{bmatrix}\right](\mathbf{I}+\Lambda_1)^{-1}\Delta_1\overline{\mathbf{P}}_1^{\mathrm{T}}\mathbf{T} \tag{48}$$

where

$$X_1(z)=\begin{bmatrix}(z+a)^{-\frac{1}{2}-\mathrm{i}\varepsilon_1}(z-a)^{-\frac{1}{2}+\mathrm{i}\varepsilon_1} & 0\\ 0 & (z+a)^{-\frac{1}{2}+\mathrm{i}\varepsilon_1}(z-a)^{-\frac{1}{2}-\mathrm{i}\varepsilon_1}\end{bmatrix} \tag{49}$$

Applying (22), the explicit expressions for $\mathbf{f}_1'(z)$, $\mathbf{f}_2'(z)$ are

$$\begin{aligned}\mathbf{f}_1'(z)&=\mathbf{C}_1^{-1}\mathbf{M}^{-1}\mathbf{P}_1\left[\mathbf{I}-X_1(z)\begin{bmatrix}z+2\mathrm{i}a\varepsilon_1 & 0\\ 0 & z-2\mathrm{i}a\varepsilon_1\end{bmatrix}\right](\mathbf{I}+\Lambda_1)^{-1}\Delta_1\overline{\mathbf{P}}_1^{\mathrm{T}}\mathbf{T}\\ \mathbf{f}_2'(z)&=\mathbf{C}_2^{-1}\overline{\mathbf{M}}^{-1}\mathbf{P}_1\left[\mathbf{I}-X_1(z)\begin{bmatrix}z+2\mathrm{i}a\varepsilon_1 & 0\\ 0 & z-2\mathrm{i}a\varepsilon_1\end{bmatrix}\right](\mathbf{I}+\Lambda_1)^{-1}\Delta_1\overline{\mathbf{P}}_1^{\mathrm{T}}\mathbf{T}\end{aligned} \tag{50}$$

Integrating (50), we arrive at expressions for $\mathbf{f}_1(z)$, $\mathbf{f}_2(z)$:

$$\begin{aligned}\mathbf{f}_1(z)&=\mathbf{C}_1^{-1}\mathbf{M}^{-1}\mathbf{P}_1[z\mathbf{I}-(z^2-a^2)X_1(z)](\mathbf{I}+\Lambda_1)^{-1}\Delta_1\overline{\mathbf{P}}_1^{\mathrm{T}}\mathbf{T}\\ \mathbf{f}_2(z)&=\mathbf{C}_2^{-1}\overline{\mathbf{M}}^{-1}\mathbf{P}_1[z\mathbf{I}-(z^2-a^2)X_1(z)](\mathbf{I}+\Lambda_1)^{-1}\Delta_1\overline{\mathbf{P}}_1^{\mathrm{T}}\mathbf{T}\end{aligned} \tag{51}$$

### 3.2. Low speed regime

It can be easily verified that the following conditions hold for the components of $\mathbf{M}$:

$$M_{11}<0,\quad M_{22}<0,\quad M_{11}M_{22}<M_{12}^2 \tag{52}$$

Then $\delta$ in (27) can be explicitly determined to be

$$\delta=-1\pm\mathrm{i}\varepsilon_2 \tag{53}$$

where

$$\varepsilon_2=\frac{1}{2\pi}\ln\frac{\lambda_2+1}{\lambda_2-1},\quad \lambda_2=\frac{M_{12}}{\sqrt{M_{11}M_{22}}}\quad(|\lambda_2|>1) \tag{54}$$

Now we introduce the following coordinate transformation:

$$\mathbf{h}(z)=\mathbf{P}_2\hat{\mathbf{h}}(z),\quad \widehat{\mathbf{T}}_2=\Delta_2\overline{\mathbf{P}}_2^{\mathrm{T}}\mathbf{T} \tag{55}$$

where

$$\mathbf{P}_2=\begin{bmatrix}\sqrt{-M_{11}} & \sqrt{-M_{11}}\\ -\mathrm{i}\sqrt{-M_{22}} & \mathrm{i}\sqrt{-M_{22}}\end{bmatrix},\quad \Delta_2=-\begin{bmatrix}1-\lambda_2 & 0\\ 0 & 1+\lambda_2\end{bmatrix} \tag{56}$$

Then (25) can be decoupled in the new coordinate system as

$$\hat{\mathbf{h}}^+(x)+\Lambda_2\hat{\mathbf{h}}^-(x)=\widehat{\mathbf{T}}_2,\quad |x|<a \tag{57}$$

where

$$\Lambda_2=-\begin{bmatrix}e^{-2\pi\varepsilon_2} & 0\\ 0 & e^{2\pi\varepsilon_2}\end{bmatrix} \tag{58}$$

Consequently, the explicit expression of $\mathbf{h}(z)$ can be obtained as

$$\mathbf{h}(z)=\mathbf{P}_2\left[\mathbf{I}-X_2(z)\begin{bmatrix}z+(2\mathrm{i}-1)a\varepsilon_2 & 0\\ 0 & z-(2\mathrm{i}+1)a\varepsilon_2\end{bmatrix}\right](\mathbf{I}+\Lambda_2)^{-1}\Delta_2\overline{\mathbf{P}}_2^{\mathrm{T}}\mathbf{T} \tag{59}$$

where

$$X_2(z)=\begin{bmatrix}(z+a)^{-i\varepsilon_2}(z-a)^{-1+i\varepsilon_2} & 0\\ 0 & (z+a)^{i\varepsilon_2}(z-a)^{-1-i\varepsilon_2}\end{bmatrix} \tag{60}$$

Applying (22), the explicit expressions for $\mathbf{f}_1'(z)$, $\mathbf{f}_2'(z)$ are

$$\begin{aligned}\mathbf{f}_1'(z)&=\mathbf{C}_1^{-1}\mathbf{M}^{-1}\mathbf{P}_2\left[\mathbf{I}-X_2(z)\begin{bmatrix}z+(2i-1)a\varepsilon_2 & 0\\ 0 & z-(2i+1)a\varepsilon_2\end{bmatrix}\right](\mathbf{I}+\Lambda_2)^{-1}\Delta_2\overline{\mathbf{P}}_2^{T}\mathbf{T}\\ \mathbf{f}_2'(z)&=\mathbf{C}_2^{-1}\overline{\mathbf{M}}^{-1}\mathbf{P}_2\left[\mathbf{I}-X_2(z)\begin{bmatrix}z+(2i-1)a\varepsilon_2 & 0\\ 0 & z-(2i+1)a\varepsilon_2\end{bmatrix}\right](\mathbf{I}+\Lambda_2)^{-1}\Delta_2\overline{\mathbf{P}}_2^{T}\mathbf{T}\end{aligned} \tag{61}$$

Integrating (61), we arrive at expressions for $\mathbf{f}_1(z)$, $\mathbf{f}_2(z)$:

$$\begin{aligned}\mathbf{f}_1(z)&=\mathbf{C}_1^{-1}\mathbf{M}^{-1}\mathbf{P}_2[z\mathbf{I}-(z^2-a^2)X_2(z)](\mathbf{I}+\Lambda_2)^{-1}\Delta_2\overline{\mathbf{P}}_2^{T}\mathbf{T}\\ \mathbf{f}_2(z)&=\mathbf{C}_2^{-1}\overline{\mathbf{M}}^{-1}\mathbf{P}_2[z\mathbf{I}-(z^2-a^2)X_2(z)](\mathbf{I}+\Lambda_2)^{-1}\Delta_2\overline{\mathbf{P}}_2^{T}\mathbf{T}\end{aligned} \tag{62}$$

### 3.3. Intermediate speed regime

In this regime, the following condition holds for the components of $\mathbf{M}$:

$$M_{11}M_{22}<0 \tag{63}$$

Then $\delta$ in (27) can be explicitly determined to be

$$\delta=-\tfrac{1}{2}\pm k \tag{64}$$

where

$$k=\frac{\tan^{-1}(\lambda_3)}{\pi},\quad \lambda_3=\frac{M_{12}}{\sqrt{-M_{11}M_{22}}} \tag{65}$$

Now we introduce the following coordinate transformation:

$$\mathbf{h}(z)=\mathbf{P}_3\hat{\mathbf{h}}(z),\quad \widehat{\mathbf{T}}_3=\Delta_3\overline{\mathbf{P}}_3^{T}\mathbf{T} \tag{66}$$

where

$$\mathbf{P}_3=\begin{bmatrix}\sqrt{-M_{11}} & \sqrt{-M_{11}}\\ \sqrt{M_{22}} & -\sqrt{M_{22}}\end{bmatrix},\quad \Delta_3=-\begin{bmatrix}0 & 1-i\lambda_3\\ 1+i\lambda_3 & 0\end{bmatrix} \tag{67}$$

Then (25) can be decoupled in the new coordinate system as

$$\hat{\mathbf{h}}^{+}(x)+\Lambda_3\hat{\mathbf{h}}^{-}(x)=\widehat{\mathbf{T}}_3,\quad |x|<a \tag{68}$$

where

$$\Lambda_3=\begin{bmatrix}e^{i2\pi k} & 0\\ 0 & e^{-i2\pi k}\end{bmatrix} \tag{69}$$

Consequently, the explicit expression of $\mathbf{h}(z)$ can be obtained as

$$\mathbf{h}(z)=\mathbf{P}_3\left[\mathbf{I}-X_3(z)\begin{bmatrix}z+2ak & 0\\ 0 & z-2ak\end{bmatrix}\right](\mathbf{I}+\Lambda_3)^{-1}\Delta_3\overline{\mathbf{P}}_3^{T}\mathbf{T} \tag{70}$$

where

$$X_3(z)=\begin{bmatrix}(z+a)^{-\frac{1}{2}-k}(z-a)^{-\frac{1}{2}+k} & 0\\ 0 & (z+a)^{-\frac{1}{2}+k}(z-a)^{-\frac{1}{2}-k}\end{bmatrix} \tag{71}$$

Applying (22), the explicit expressions for $\mathbf{f}_1'(z)$, $\mathbf{f}_2'(z)$ are

$$\begin{aligned}\mathbf{f}_1'(z)&=\mathbf{C}_1^{-1}\mathbf{M}^{-1}\mathbf{P}_3\left[\mathbf{I}-X_3(z)\begin{bmatrix}z+2ak & 0\\ 0 & z-2ak\end{bmatrix}\right](\mathbf{I}+\Lambda_3)^{-1}\Delta_3\overline{\mathbf{P}}_3^{\mathrm{T}}\mathbf{T}\\ \mathbf{f}_2'(z)&=\mathbf{C}_2^{-1}\overline{\mathbf{M}}^{-1}\mathbf{P}_3\left[\mathbf{I}-X_3(z)\begin{bmatrix}z+2ak & 0\\ 0 & z-2ak\end{bmatrix}\right](\mathbf{I}+\Lambda_3)^{-1}\Delta_3\overline{\mathbf{P}}_3^{\mathrm{T}}\mathbf{T}\end{aligned} \tag{72}$$

Integrating (72), we arrive at expressions for $\mathbf{f}_1(z)$, $\mathbf{f}_2(z)$:

$$\begin{aligned}\mathbf{f}_1(z)&=\mathbf{C}_1^{-1}\mathbf{M}^{-1}\mathbf{P}_3[z\mathbf{I}-(z^2-a^2)X_3(z)](\mathbf{I}+\Lambda_3)^{-1}\Delta_3\overline{\mathbf{P}}_3^{\mathrm{T}}\mathbf{T}\\ \mathbf{f}_2(z)&=\mathbf{C}_2^{-1}\overline{\mathbf{M}}^{-1}\mathbf{P}_3[z\mathbf{I}-(z^2-a^2)X_3(z)](\mathbf{I}+\Lambda_3)^{-1}\Delta_3\overline{\mathbf{P}}_3^{\mathrm{T}}\mathbf{T}\end{aligned} \tag{73}$$

### 3.4. High speed regime

It can be easily verified that the following conditions hold for the components of $\mathbf{M}$:

$$M_{11}>0,\quad M_{22}>0,\quad M_{11}M_{22}<M_{12}^2 \tag{74}$$

Then $\delta$ in (27) can be explicitly determined to be

$$\delta=-1\pm\mathrm{i}\varepsilon_3 \tag{75}$$

where

$$\varepsilon_3=\frac{1}{2\pi}\ln\frac{\lambda_4+1}{\lambda_4-1},\quad \lambda_4=\frac{M_{12}}{\sqrt{M_{11}M_{22}}}\quad(|\lambda_4|>1) \tag{76}$$

Now we introduce the following coordinate transformation:

$$\mathbf{h}(z)=\mathbf{P}_4\hat{\mathbf{h}}(z),\quad \widehat{\mathbf{T}}_2=\Delta_4\overline{\mathbf{P}}_4^{\mathrm{T}}\mathbf{T} \tag{77}$$

where

$$\mathbf{P}_4=\begin{bmatrix}\sqrt{M_{11}} & \sqrt{M_{11}}\\ \mathrm{i}\sqrt{M_{22}} & -\mathrm{i}\sqrt{M_{22}}\end{bmatrix},\quad \Delta_2=\begin{bmatrix}1-\lambda_4 & 0\\ 0 & 1+\lambda_4\end{bmatrix} \tag{78}$$

Then (25) can be decoupled in the new coordinate system as

$$\hat{\mathbf{h}}^+(x)+\Lambda_4\hat{\mathbf{h}}^-(x)=\widehat{\mathbf{T}}_4,\quad |x|<a \tag{79}$$

where

$$\Lambda_4=-\begin{bmatrix}e^{-2\pi\varepsilon_3} & 0\\ 0 & e^{2\pi\varepsilon_3}\end{bmatrix} \tag{80}$$

Consequently, the explicit expression of $\mathbf{h}(z)$ can be obtained as

$$\mathbf{h}(z)=\mathbf{P}_4\left[\mathbf{I}-X_4(z)\begin{bmatrix}z+(2\mathrm{i}+1)a\varepsilon_3 & 0\\ 0 & z-(2\mathrm{i}-1)a\varepsilon_3\end{bmatrix}\right](\mathbf{I}+\Lambda_4)^{-1}\Delta_4\overline{\mathbf{P}}_4^{\mathrm{T}}\mathbf{T} \tag{81}$$

where

$$X_4(z) = \begin{bmatrix} (z+a)^{-i\varepsilon_3}(z-a)^{-1+i\varepsilon_3} & 0 \\ 0 & (z+a)^{i\varepsilon_3}(z-a)^{-1-i\varepsilon_3} \end{bmatrix} \tag{82}$$

Applying (22), the explicit expressions for $\mathbf{f}_1'(z)$, $\mathbf{f}_2'(z)$ are

$$\begin{aligned} \mathbf{f}_1'(z) &= \mathbf{C}_1^{-1}\mathbf{M}^{-1}\mathbf{P}_4\left[\mathbf{I} - X_4(z)\begin{bmatrix} z+(2i+1)a\varepsilon_3 & 0 \\ 0 & z-(2i-1)a\varepsilon_3 \end{bmatrix}\right](\mathbf{I}+\Lambda_4)^{-1}\Delta_4\overline{\mathbf{P}}_4^{\mathrm{T}}\mathbf{T} \\ \mathbf{f}_2'(z) &= \mathbf{C}_2^{-1}\overline{\mathbf{M}}^{-1}\mathbf{P}_4\left[\mathbf{I} - X_4(z)\begin{bmatrix} z+(2i+1)a\varepsilon_3 & 0 \\ 0 & z-(2i-1)a\varepsilon_3 \end{bmatrix}\right](\mathbf{I}+\Lambda_4)^{-1}\Delta_4\overline{\mathbf{P}}_4^{\mathrm{T}}\mathbf{T} \end{aligned} \tag{83}$$

Integrating (83), we arrive at expressions for $\mathbf{f}_1(z)$, $\mathbf{f}_2(z)$

$$\begin{aligned} \mathbf{f}_1(z) &= \mathbf{C}_1^{-1}\mathbf{M}^{-1}\mathbf{P}_4[z\mathbf{I} - (z^2-a^2)X_2(z)](\mathbf{I}+\Lambda_4)^{-1}\Delta_4\overline{\mathbf{P}}_4^{\mathrm{T}}\mathbf{T} \\ \mathbf{f}_2(z) &= \mathbf{C}_2^{-1}\overline{\mathbf{M}}^{-1}\mathbf{P}_4[z\mathbf{I} - (z^2-a^2)X_2(z)](\mathbf{I}+\Lambda_4)^{-1}\Delta_4\overline{\mathbf{P}}_4^{\mathrm{T}}\mathbf{T} \end{aligned} \tag{84}$$

It is observed that the nature of the singularities in this speed regime is the same as that in the low speed regime.

### 3.5. Extremely high speed regime

It can be easily checked that the following conditions hold for the components of $\mathbf{M}$:

$$M_{11} < 0, \quad M_{22} < 0, \quad M_{11}M_{22} > M_{12}^2 \tag{85}$$

Then $\delta$ in (27) can be explicitly determined to be

$$\delta = -\tfrac{1}{2} \pm i\varepsilon_4 \tag{86}$$

where

$$\varepsilon_4 = \frac{1}{2\pi}\ln\frac{1+\lambda_5}{1-\lambda_5}, \quad \lambda_5 = \frac{M_{12}}{\sqrt{M_{11}M_{22}}} \quad (|\lambda_1| < 1) \tag{87}$$

Now we introduce the following coordinate transformation:

$$\mathbf{h}(z) = \mathbf{P}_5\hat{\mathbf{h}}(z), \quad \widehat{\mathbf{T}}_1 = \Delta_5\overline{\mathbf{P}}_5^{\mathrm{T}}\mathbf{T} \tag{88}$$

where

$$\mathbf{P}_5 = \begin{bmatrix} \sqrt{-M_{11}} & \sqrt{-M_{11}} \\ -i\sqrt{-M_{22}} & i\sqrt{-M_{22}} \end{bmatrix}, \quad \Delta_5 = -\begin{bmatrix} 1-\lambda_5 & 0 \\ 0 & 1+\lambda_5 \end{bmatrix} \tag{89}$$

Then (25) can be decoupled in the new coordinate system as

$$\hat{\mathbf{h}}^+(x) + \Lambda_5\hat{\mathbf{h}}^-(x) = \widehat{\mathbf{T}}_5, \quad |x| < a \tag{90}$$

where

$$\Lambda_5 = \begin{bmatrix} e^{-2\pi\varepsilon_4} & 0 \\ 0 & e^{2\pi\varepsilon_4} \end{bmatrix} \tag{91}$$

Consequently, the explicit expression of $\mathbf{h}(z)$ can be obtained as

$$\mathbf{h}(z)=\mathbf{P}_5\left[\mathbf{I}-X_5(z)\begin{bmatrix} z+2\mathrm{i}a\varepsilon_4 & 0\\ 0 & z-2\mathrm{i}a\varepsilon_4\end{bmatrix}\right](\mathbf{I}+\Lambda_5)^{-1}\Delta_5\overline{\mathbf{P}}_5^{\mathrm{T}}\mathbf{T} \tag{92}$$

where

$$X_5(z)=\begin{bmatrix}(z+a)^{-\frac{1}{2}-\mathrm{i}\varepsilon_4}(z-a)^{-\frac{1}{2}+\mathrm{i}\varepsilon_4} & 0\\ 0 & (z+a)^{-\frac{1}{2}+\mathrm{i}\varepsilon_4}(z-a)^{-\frac{1}{2}-\mathrm{i}\varepsilon_4}\end{bmatrix} \tag{93}$$

Applying (22), the explicit expressions for $\mathbf{f}_1'(z)$, $\mathbf{f}_2'(z)$ are

$$\begin{aligned}\mathbf{f}_1'(z)&=\mathbf{C}_1^{-1}\mathbf{M}^{-1}\mathbf{P}_5\left[\mathbf{I}-X_5(z)\begin{bmatrix} z+2\mathrm{i}a\varepsilon_4 & 0\\ 0 & z-2\mathrm{i}a\varepsilon_4\end{bmatrix}\right](\mathbf{I}+\Lambda_5)^{-1}\Delta_5\overline{\mathbf{P}}_5^{\mathrm{T}}\mathbf{T}\\ \mathbf{f}_2'(z)&=\mathbf{C}_2^{-1}\overline{\mathbf{M}}^{-1}\mathbf{P}_5\left[\mathbf{I}-X_5(z)\begin{bmatrix} z+2\mathrm{i}a\varepsilon_4 & 0\\ 0 & z-2\mathrm{i}a\varepsilon_4\end{bmatrix}\right](\mathbf{I}+\Lambda_5)^{-1}\Delta_5\overline{\mathbf{P}}_5^{\mathrm{T}}\mathbf{T}\end{aligned} \tag{94}$$

Integrating (94), we arrive at expressions for $\mathbf{f}_1(z)$, $\mathbf{f}_2(z)$:

$$\begin{aligned}\mathbf{f}_1(z)&=\mathbf{C}_1^{-1}\mathbf{M}^{-1}\mathbf{P}_5[z\mathbf{I}-(z^2-a^2)X_5(z)](\mathbf{I}+\Lambda_5)^{-1}\Delta_5\overline{\mathbf{P}}_5^{\mathrm{T}}\mathbf{T}\\ \mathbf{f}_2(z)&=\mathbf{C}_2^{-1}\overline{\mathbf{M}}^{-1}\mathbf{P}_5[z\mathbf{I}-(z^2-a^2)X_5(z)](\mathbf{I}+\Lambda_5)^{-1}\Delta_5\overline{\mathbf{P}}_5^{\mathrm{T}}\mathbf{T}\end{aligned} \tag{95}$$

It is observed that the nature of the singularities in this speed regime is the same as that in the extremely low speed regime.

## 4. Field components on the interface

The exact solution derived in the previous section can be expediently applied to extract field components on the interface, which are listed for extremely low speed regime as follows:

- $\sigma_{32}$ and $E_1$ along the interface

$$\begin{aligned}\begin{bmatrix}\sigma_{32}\\ -E_1\end{bmatrix}^+&=\begin{bmatrix}\sigma_{32}\\ -E_1\end{bmatrix}^-\\ &=\frac{1}{M_{11}M_{22}-M_{12}^2}\begin{bmatrix}M_{11} & 0\\ 0 & M_{22}\end{bmatrix}\mathbf{P}_1\left[\mathbf{I}-X_1(x)\begin{bmatrix}x+2\mathrm{i}a\varepsilon_1 & 0\\ 0 & x-2\mathrm{i}a\varepsilon_1\end{bmatrix}\right](\mathbf{I}+\Lambda_1)^{-1}\Delta_1\overline{\mathbf{P}}_1^{\mathrm{T}}\mathbf{T},\quad |x|\geqslant a\end{aligned} \tag{96}$$

- $\sigma_{31}$ and $E_2$ along the interface

$$\begin{aligned}\begin{bmatrix}\sigma_{31}\\ E_2\end{bmatrix}^+=\mathrm{Im}\left\{\begin{bmatrix}\bar{c}_{44}^{(1)} & \mathrm{i}\frac{e_{15}^{(1)}}{\varepsilon_{11}^{(1)}}\\ -\mathrm{i}\beta^{(1)}\frac{e_{15}^{(1)}}{\varepsilon_{11}^{(1)}} & \frac{1}{\varepsilon_{11}^{(1)}}\end{bmatrix}\mathbf{C}_1^{-1}\mathbf{M}^{-1}\mathbf{P}_1\left[\mathbf{I}-X_1^+(x)\begin{bmatrix}x+2\mathrm{i}a\varepsilon_1 & 0\\ 0 & x-2\mathrm{i}a\varepsilon_1\end{bmatrix}\right](\mathbf{I}+\Lambda_1)^{-1}\Delta_1\overline{\mathbf{P}}_1^{\mathrm{T}}\mathbf{T}\right\},\\ -\infty<x<+\infty\end{aligned} \tag{97a}$$

$$\begin{bmatrix}\sigma_{31}\\ E_2\end{bmatrix}^- = \mathrm{Im}\left\{\begin{bmatrix}\bar{c}_{44}^{(2)} & \mathrm{i}\frac{e_{15}^{(2)}}{\varepsilon_{11}^{(2)}}\\ -\mathrm{i}\beta^{(2)}\frac{e_{15}^{(2)}}{\varepsilon_{11}^{(2)}} & \frac{1}{\varepsilon_{11}^{(2)}}\end{bmatrix}\mathbf{C}_2^{-1}\overline{\mathbf{M}}^{-1}\mathbf{P}_1\left[\mathbf{I}-X_1^-(x)\begin{bmatrix}x+2\mathrm{i}a\varepsilon_1 & 0\\ 0 & x-2\mathrm{i}a\varepsilon_1\end{bmatrix}\right](\mathbf{I}+\Lambda_1)^{-1}\Delta_1\overline{\mathbf{P}}_1^{\mathrm{T}}\mathbf{T}\right\},\quad -\infty<x<+\infty \tag{97b}$$

- $\gamma_{31}$ and $D_2$ along the interface

$$\begin{bmatrix}\gamma_{31}\\ D_2\end{bmatrix}^+ = \mathrm{Im}\left\{\mathbf{C}_1^{-1}\mathbf{M}^{-1}\mathbf{P}_1\left[\mathbf{I}-X_1^+(x)\begin{bmatrix}x+2\mathrm{i}a\varepsilon_1 & 0\\ 0 & x-2\mathrm{i}a\varepsilon_1\end{bmatrix}\right](\mathbf{I}+\Lambda_1)^{-1}\Delta_1\overline{\mathbf{P}}_1^{\mathrm{T}}\mathbf{T}\right\},\quad -\infty<x<+\infty \tag{98a}$$

$$\begin{bmatrix}\gamma_{31}\\ D_2\end{bmatrix}^- = \mathrm{Im}\left\{\mathbf{C}_1^{-1}\overline{\mathbf{M}}^{-1}\mathbf{P}_1\left[\mathbf{I}-X_1^-(x)\begin{bmatrix}x+2\mathrm{i}a\varepsilon_1 & 0\\ 0 & x-2\mathrm{i}a\varepsilon_1\end{bmatrix}\right](\mathbf{I}+\Lambda_1)^{-1}\Delta_1\overline{\mathbf{P}}_1^{\mathrm{T}}\mathbf{T}\right\},\quad -\infty<x<+\infty \tag{98b}$$

- Discontinuity in $w$ and $\varphi$ over the crack surfaces

$$\begin{bmatrix}w^{(1)}(x,0^+)-w^{(2)}(x,0^-)\\ \varphi^{(1)}(x,0^+)-\varphi^{(2)}(x,0^-)\end{bmatrix} = -\frac{\mathrm{i}}{2}(x^2-a^2)\mathbf{P}_1X_1^+(x)\Lambda_1^{-1}\Delta_1\overline{\mathbf{P}}_1^{\mathrm{T}}\mathbf{T},\quad |x|<a \tag{99}$$

Differentiating (99) with respect to the $x$-axis, then densities of screw dislocations and electric charges are distributed on the crack faces as follows:

$$\begin{bmatrix}\hat{b}\\ \hat{q}\end{bmatrix} = \frac{\mathrm{i}}{2}\mathbf{P}_1X_1^+(x)\begin{bmatrix}x+2\mathrm{i}a\varepsilon_1 & 0\\ 0 & x-2\mathrm{i}a\varepsilon_1\end{bmatrix}\Lambda_1^{-1}\Delta_1\overline{\mathbf{P}}_1^{\mathrm{T}}\mathbf{T},\quad |x|<a \tag{100}$$

## 5. Results and discussions

### 5.1. A conducting crack moving in a homogeneous piezoelectric material

In this case $\mathbf{C}_1=\mathbf{C}_2=\mathbf{C}$, as a result $\delta=-1/2$. The analytic functions $\mathbf{f}_1'(z)$, $\mathbf{f}_2'(z)$ defined in the upper and lower half planes are

$$\mathbf{f}_1'(z)=\mathbf{f}_2'(z)=\mathbf{C}^{-1}\mathbf{T}\left(1-\frac{z}{\sqrt{z^2-a^2}}\right) \tag{101}$$

Tractions and tangential electric field are distributed on the real axis as follows:

$$\begin{bmatrix}\sigma_{32}\\ E_1\end{bmatrix} = \left(\frac{|x|}{\sqrt{x^2-a^2}}-1\right)\begin{bmatrix}\sigma_{32}^{\infty}\\ E_1^{\infty}\end{bmatrix},\quad |x|>a \tag{102}$$

The stresses and electric fields exhibit inverse square root singularities near the crack tips. Then the intensity factors for stresses and electric fields can be defined as

$$K_\sigma = \lim_{x\to a}\sqrt{2\pi(x-a)}\sigma_{32}(x,0) = \sigma_{32}^{\infty}\sqrt{\pi a}$$
$$K_E = \lim_{x\to a}\sqrt{2\pi(x-a)}E_1(x,0) = E_1^{\infty}\sqrt{\pi a} \tag{103}$$

which are just identical to Yoffe's results (Yoffe, 1951). Discontinuity in $w$ and $\varphi$ over the crack surfaces can be expressed as

$$\Delta w(x) = w^{(1)}(x,0^+) - w^{(2)}(x,0^-) = \frac{\sigma_{32}^{\infty}}{\bar{c}_{44}(\beta - k_e^2)}\sqrt{a^2-x^2},$$
$$\Delta\varphi(x) = \varphi^{(1)}(x,0^+) - \varphi^{(2)}(x,0^-) = -\frac{E_1^{\infty}\varepsilon_{11}\beta}{\beta - k_e^2}\sqrt{a^2-x^2}, \qquad |x| < a \tag{104}$$

It is observed from (104) that when the moving velocity is very near the Bleustein–Gulyaev velocity, the magnitude of $\Delta w$ and $\Delta\varphi$ will become considerably large. The asymptotic electroelastic fields near the right crack tip can be expressed as

$$\sigma_{31} = \frac{1}{\beta - k_e^2}\frac{e_{15}K_E}{\sqrt{2\pi\tilde{r}}}\cos(\tilde{\theta}/2) - \frac{\beta}{\beta - k_e^2}\frac{e_{15}K_E}{\sqrt{2\pi r}}\cos(\theta/2) - \frac{1}{\beta - k_e^2}\frac{K_\sigma}{\sqrt{2\pi\tilde{r}}}\sin(\tilde{\theta}/2) + \frac{k_e^2}{\beta - k_e^2}\frac{K_\sigma}{\sqrt{2\pi r}}\sin(\theta/2) \tag{105}$$

$$\sigma_{32} = \frac{\beta}{\beta - k_e^2}\frac{K_\sigma}{\sqrt{2\pi\tilde{r}}}\cos(\tilde{\theta}/2) - \frac{k_e^2}{\beta - k_e^2}\frac{K_\sigma}{\sqrt{2\pi r}}\cos(\theta/2) + \frac{\beta}{\beta - k_e^2}\frac{e_{15}K_E}{\sqrt{2\pi\tilde{r}}}\sin(\tilde{\theta}/2) - \frac{\beta}{\beta - k_e^2}\frac{e_{15}K_E}{\sqrt{2\pi r}}\sin(\theta/2) \tag{106}$$

$$\gamma_{31} = \frac{1}{\beta - k_e^2}\frac{e_{15}K_E}{\bar{c}_{44}}\frac{\cos(\tilde{\theta}/2)}{\sqrt{2\pi\tilde{r}}} - \frac{1}{\beta - k_e^2}\frac{K_\sigma}{\bar{c}_{44}}\frac{\sin(\tilde{\theta}/2)}{\sqrt{2\pi\tilde{r}}} \tag{107}$$

$$\gamma_{32} = \frac{\beta}{\beta - k_e^2}\frac{K_\sigma}{\bar{c}_{44}}\frac{\cos(\tilde{\theta}/2)}{\sqrt{2\pi\tilde{r}}} + \frac{\beta}{\beta - k_e^2}\frac{e_{15}K_E}{\bar{c}_{44}}\frac{\sin(\tilde{\theta}/2)}{\sqrt{2\pi\tilde{r}}} \tag{108}$$

$$D_1 = \frac{\beta}{\beta - k_e^2}\varepsilon_{11}K_E\frac{\cos(\theta/2)}{\sqrt{2\pi r}} - \frac{1}{\beta - k_e^2}\frac{e_{15}K_\sigma}{\bar{c}_{44}}\frac{\sin(\theta/2)}{\sqrt{2\pi r}} \tag{109}$$

$$D_2 = \frac{1}{\beta - k_e^2}\frac{e_{15}K_\sigma}{\bar{c}_{44}}\frac{\cos(\theta/2)}{\sqrt{2\pi r}} + \frac{\beta}{\beta - k_e^2}\varepsilon_{11}K_E\frac{\sin(\theta/2)}{\sqrt{2\pi r}} \tag{110}$$

$$E_1 = -\frac{k_e^2}{\beta - k_e^2}\frac{K_E}{\sqrt{2\pi\tilde{r}}}\cos(\tilde{\theta}/2) + \frac{\beta}{\beta - k_e^2}\frac{K_E}{\sqrt{2\pi r}}\cos(\theta/2) + \frac{k_e^2}{\beta - k_e^2}\frac{K_\sigma}{e_{15}\sqrt{2\pi\tilde{r}}}\sin(\tilde{\theta}/2) - \frac{k_e^2}{\beta - k_e^2}\frac{K_\sigma}{e_{15}\sqrt{2\pi r}}\sin(\theta/2) \tag{111}$$

$$E_2 = -\frac{\beta k_e^2}{\beta - k_e^2}\frac{K_\sigma}{e_{15}\sqrt{2\pi\tilde{r}}}\cos(\tilde{\theta}/2) + \frac{k_e^2}{\beta - k_e^2}\frac{K_\sigma}{e_{15}\sqrt{2\pi r}}\cos(\theta/2) - \frac{\beta k_e^2}{\beta - k_e^2}\frac{K_E}{\sqrt{2\pi\tilde{r}}}\sin(\tilde{\theta}/2) + \frac{\beta}{\beta - k_e^2}\frac{K_E}{\sqrt{2\pi r}}\sin(\theta/2) \tag{112}$$

where

$$r = \sqrt{(x-a)^2 + y^2}, \quad \theta = \tan^{-1}\left(\frac{y}{x-a}\right)$$
$$\tilde{r} = \sqrt{(x-a)^2 + (\beta y)^2}, \quad \tilde{\theta} = \tan^{-1}\left(\frac{\beta y}{x-a}\right) \tag{113}$$

It is observed from (110) that the intensity factor for electric displacement is

$$K_D = \lim_{x\to a}\sqrt{2\pi(x-a)}D_2(x,0) = \frac{e_{15}\sigma_{32}^{\infty}\sqrt{\pi a}}{\bar{c}_{44}(\beta - k_e^2)} \tag{114}$$

Then $K_D$ goes to infinity when $\beta = k_e^2$ or $V = c_{\mathrm{bg}}$.

### 5.2. A conducting crack moving at the interface of two dissimilar piezoelectric materials

#### 5.2.1. Speed regimes

The electroelastic constants for several commonly used piezoelectric materials are tabulated in Table 1. The corresponding electroacoustic constants of these piezoelectric materials are shown in Table 2. It shall be indicated that the bulk shear wave speeds for PZT65/35 and ZnO calculated by Li and Mataga (1996) are incorrect. Table 3 presents two velocity parameters $V_1$ and $V_2$ for all of the possible material combinations from the six piezoelectric materials. Observing Tables 2 and 3, we find that there exist only the first two speed regimes for the piezoelectric composites PZT65/35 + ZnO and PZT-5 + ZnO. There exist the first three speed regimes for the piezoelectric composites PZT65/35 + $BaTiO_3$, PZT-5 + $BaTiO_3$, and $BaTiO_3$ + ZnO. There exist the first four speed regimes for the piezoelectric composites PZT65/35 + PZT-5, PZT-5 + PZT-5H, PZT-4 + $BaTiO_3$, PZT-4 + ZnO, PZT-5H + $BaTiO_3$, and PZT-5H + ZnO. There exist all the five speed regimes for the piezoelectric composites PZT65/35 + PZT-4, PZT65/35 + PZT-5H, PZT-5 + PZT-4, and PZT-4 + PZT-5H. In the next subsection, the piezoelectric composite PZT-4 + PZT-5H, which possesses all the five speed regimes, will be taken as a typical example to demonstrate the effect of moving velocity on the singularities.

#### 5.2.2. Singularities

Fig. 2 illustrates the effect of crack moving velocity $V$ on the singularities for piezoelectric composite PZT-4 + PZT-5H. The five speed regimes are separated by vertical dashed lines. When the crack moving velocity increases within the *extremely low speed regime*, i.e., $0 \leqslant V \leqslant 2257.9$ m/s, the magnitude of the oscillatory index $\varepsilon_1$ for the singularities $-1/2 \pm i\varepsilon_1$ will monotonically increase from 0.00296, just the value for a static interface conducting crack (Wang and Zhong, 2002), to infinity. When the crack moving velocity increases within the *low speed regime*, i.e., $2257.9 < V \leqslant 2333.9$ m/s, the magnitude of the oscillatory index $\varepsilon_2$ for the singularities $-1 \pm i\varepsilon_2$ will monotonically decrease from infinity to zero. When the

Table 1
Material properties for several piezoelectric ceramics

| Compound | $c_{44}$ ($10^{10}$ N/m$^2$) | $e_{15}$ (C/m$^2$) | $\varepsilon_{11}$ ($10^{-9}$ F/m) | $\rho$ ($10^3$ kg/m$^3$) |
|---|---|---|---|---|
| PZT65/35 | 3.890 | 8.387 | 5.66 | 7.825 |
| PZT-5 | 2.11 | 12.3 | 8.1103 | 7.75 |
| PZT-4 | 2.56 | 12.7 | 6.4634 | 7.5 |
| PZT-5H | 3.53 | 17.0 | 15.1 | 7.5 |
| $BaTiO_3$ | 4.4 | 11.4 | 9.8722 | 5.7 |
| ZnO | 4.247 | −0.48 | 0.0757 | 5.68 |

Table 2
Electroacoustic constants of several piezoelectric ceramics

| Compound | $\bar{c}_{44}$ ($10^{10}$ N/m$^2$) | $k_e$ | $s$ (m/s) | $c_{bg}$ (m/s) |
|---|---|---|---|---|
| PZT65/35 | 5.1328 | 0.4921 | 2561.1 | 2484.9 |
| PZT-5 | 3.9754 | 0.6850 | 2264.9 | 2000.0 |
| PZT-4 | 5.0554 | 0.7026 | 2596.3 | 2257.9 |
| PZT-5H | 5.4439 | 0.5959 | 2694.2 | 2522.2 |
| $BaTiO_3$ | 5.7164 | 0.4799 | 3166.8 | 3081.7 |
| ZnO | 4.5514 | 0.2586 | 2830.7 | 2824.4 |

Table 3
$V_1$ and $V_2$ of several piezoelectric composites (the first one is $V_1$, and the second one is $V_2$ in each element, unit m/s)

| | PZT65/35 | PZT-5 | PZT-4 | PZT-5H | $BaTiO_3$ |
|---|---|---|---|---|---|
| PZT-5 | 2183.7 | | | | |
| | 2237.9 | | | | |
| PZT-4 | 2409.6 | 2088.3 | | | |
| | 2398.2 | 2114.1 | | | |
| PZT-5H | 2489.4 | 2095.5 | 2333.9 | | |
| | 2499.1 | 2227.7 | 2399.1 | | |
| $BaTiO_3$ | 2519.9 | 2160.3 | 2434.1 | 2647.0 | |
| | 2561.1 | 2264.9 | 2583.3 | 2692.0 | |
| ZnO | 2561.1 | 2264.8 | 2596.2 | 2694.2 | 2824.4 |
| | 2561.1 | 2264.9 | 2559.0 | 2671.1 | 2830.7 |

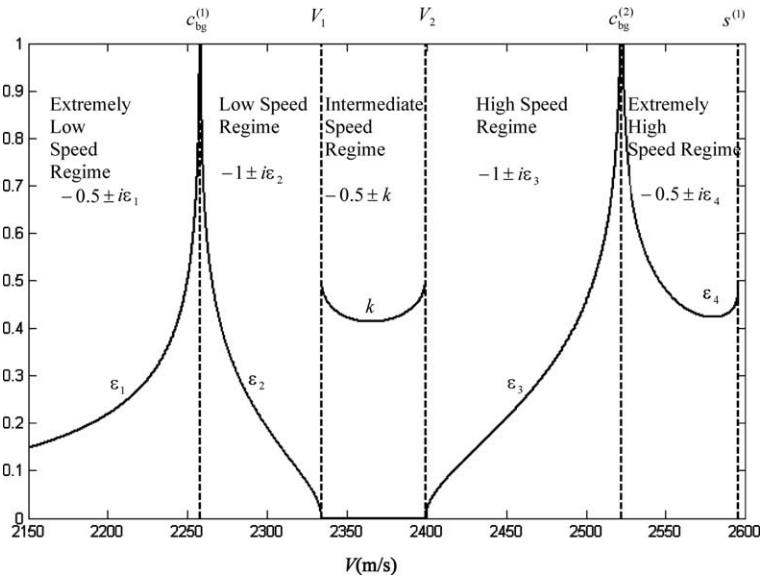


Fig. 2. The effect of crack moving velocity on the singularities for piezoelectric composite PZT-4 + PZT-5H (the upper half-plane is PZT-4, the lower is PZT-5H).

crack moving velocity increases within the *intermediate speed regime*, i.e., $2333.9 < V \leqslant 2399.1$ m/s, the magnitude of $k$ for the singularities $-1/2 \pm k$ will first decrease from 0.5 to 0.4136 for $V \leqslant 2365.2$ m/s; then it will increase from 0.4136 to 0.5 for $V > 2365.2$ m/s. When the crack moving velocity increases within the

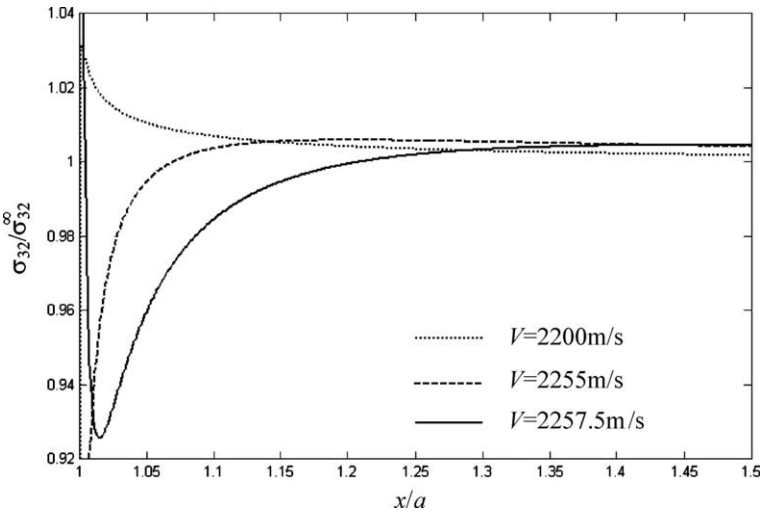


Fig. 3. $\sigma_{32}$ just ahead of the right crack tip for three different crack velocities.

*high speed regime*, i.e., $2399.1 < V \leqslant 2522.2$ m/s, the magnitude of the oscillatory index $\varepsilon_3$ for the singularities $-1 \pm i\varepsilon_3$ will monotonically increase from zero to infinity. When the crack moving velocity increases within the *extremely high speed regime*, i.e., $2522.2 < V \leqslant 2596.3$ m/s, the magnitude of the oscillatory index $\varepsilon_4$ for the singularities $-1/2 \pm i\varepsilon_4$ will first steeply decrease from infinity to 0.4234 for $V \leqslant 2580.4$ m/s; then it will gently increase from 0.4234 to 0.4846 for $V > 2580.4$ m/s.

### 5.2.3. Electroelastic field on the interface

In this subsection, the material combination of PZT-4 + PZT-5H is also taken as an illustrative example and only the extremely low speed regime $0 \leqslant V \leqslant 2257.9$ m/s is considered. The loading conditions are

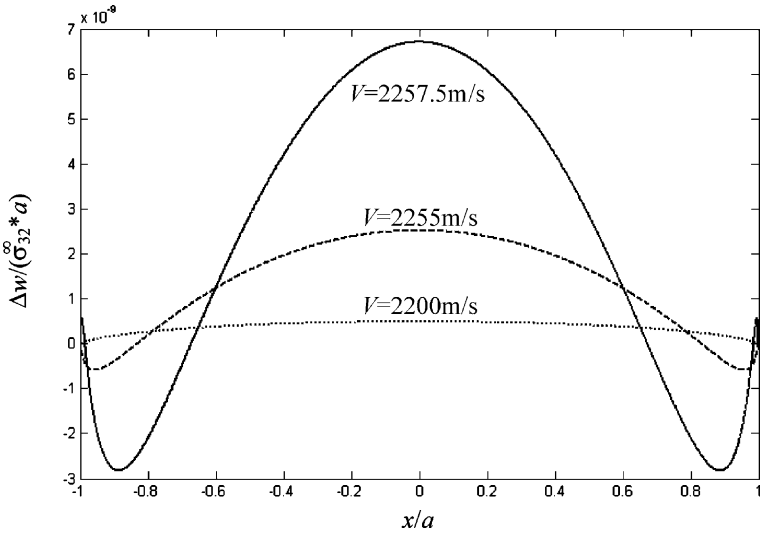


Fig. 4. Crack opening displacement $\Delta w$ for three different crack velocities.

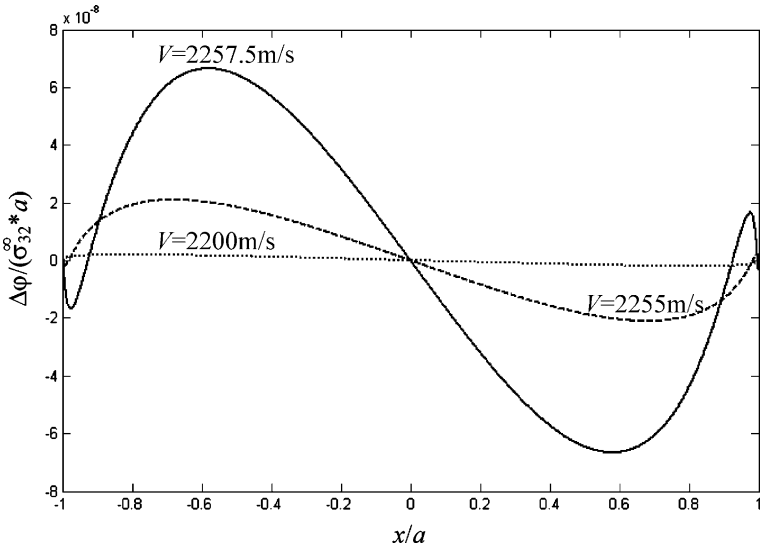


Fig. 5. $\Delta\varphi = \varphi(x,0^+) - \varphi(x,0^-)$ for three different crack velocities.

$\mathbf{T} = \begin{bmatrix} -\sigma_{32}^{\infty} \\ 0 \end{bmatrix}$. Fig. 3 demonstrates the stress component $\sigma_{32}$ just ahead of the right crack tip for three different crack velocities. It is observed that the stress oscillation becomes noticeable when the velocity is very near the Bleustein–Gulyaev velocity $c_{\mathrm{bg}}^{(1)} = 2257.9$ m/s of PZT-4. Figs. 4 and 5 illustrate crack opening displacement $\Delta w$ and $\Delta\varphi = \varphi(x,0^+) - \varphi(x,0^-)$ for the three different crack velocities. It is found that the magnitude of $\Delta w$ and $\Delta\varphi$ will become relatively large when $V \to c_{\mathrm{bg}}^{(1)} = 2257.9$ m/s. $\Delta w$ and $\Delta\varphi$ can be negative as well as positive when $V \to c_{\mathrm{bg}}^{(1)} = 2257.9$ m/s, also reflecting the serious oscillatory characteristics near the crack tips. It is observed from Fig. 5 that $\Delta\varphi \neq 0$ even though $E_1^{\infty} = 0$, an exhibition of the piezoelectric effect of the bimaterials. Noticing that the derivative of $\Delta\varphi$ with respect to $x$ is the density of electric charges distributed on the crack faces, it can then be deduced from Fig. 5 that both positive and negative electric charges are distributed on the crack faces.

## 6. Conclusions

A Yoffe-type conducting crack moving at the interface of two dissimilar piezoelectric materials is investigated. In the extremely low speed regime, the field components will exhibit the oscillatory singularities $\delta = -1/2 \pm \mathrm{i}\varepsilon_1$ near the crack tips; in the low speed regime, the field components will exhibit the singularities $\delta = -1 \pm \mathrm{i}\varepsilon_2$ near the crack tips; in the intermediate speed regime, the field components will exhibit the real power type singularities $\delta = -1/2 \pm k$ near the crack tips; in the high speed regime, the field components will exhibit the singularities $\delta = -1 \pm \mathrm{i}\varepsilon_3$ near the crack tips; in the extremely high speed regime, the field components will exhibit the oscillatory singularities $\delta = -1/2 \pm \mathrm{i}\varepsilon_4$ near the crack tips. This phenomenon, in which the nature of the singularities relies on the crack moving velocity, is different from the case of a moving insulating crack (Chen et al., 1998; Chen and Yu, 1999) or a moving permeable crack (Li et al., 2000), in which stresses, strains, electric displacements, and electric fields possess the inverse square root singularities near the crack tips. When a conducting crack runs in a homogeneous piezoelectric material, the traditionally defined stress and electric field intensity factors are introduced to describe the

singular field near the crack tips. It is found that stress and electric field intensity factors are independent of moving velocity and the material constants, while the electric displacement intensity factor is dependent on moving velocity and the material constants. The numerical results illustrate how the singularities at the crack tips are varied as the crack moving velocity increases, and shows that field components will exhibit violent oscillatory characteristics when $V \to \min\{c_{\mathrm{bg}}^{(1)}, c_{\mathrm{bg}}^{(2)}\}$.

## Acknowledgements

The authors would like to thank the reviewers for their constructive suggestions. This work was supported by the National Excellent Young Scholar Science Fund of China (Project no. 10125209), the National Natural Science Foundation of China (Project no. 10072041) and the Teaching and Research Award Fund for Outstanding Young Teachers in High Education Institutions of MOE, PR China.

## References

Bleustein, J.L., 1968. A new surface wave in piezoelectric materials. Appl. Phys. Lett. 13, 412–413.

Chen, Z.T., Yu, S.W., 1997. Antiplane Yoffe crack problem in piezoelectric materials. Int. J. Fract. 84, L41–L45.

Chen, Z.T., Yu, S.W., 1999. Anti-plane crack moving along the interface of dissimilar piezoelectric materials. Acta Mech. Solida Sinica 20, 77–81 (in Chinese).

Chen, Z.T., Karihaloo, B.L., Yu, S.W., 1998. A Griffith crack moving along the interface of dissimilar piezoelectric materials. Int. J. Fract. 91, 197–203.

Gulyaev, Y.V., 1969. Electroacoustic surface waves in solids. Sov. Phys. JETP 9, 37–38.

Kwon, J.H., Lee, K.Y., Kwon, S.M., 2000. Moving crack in a piezoelectric ceramic strip under anti-plane shear loading. Mech. Res. Commun. 27, 327–332.

Li, S., Mataga, P.A., 1996. Dynamic crack propagation in piezoelectric materials— Part I. Electrode solution. J. Mech. Phys. Solids 44, 1799–1830.

Li, C., Weng, G.J., 2002. Yoffe-type moving crack in a functionally graded piezoelectric material. Proc. Roy. Soc. Lond. A 458, 381–399.

Li, X.F., Fan, T.Y., Wu, X.F., 2000. A Moving mode-III crack at the interface between two dissimilar piezoelectric materials. Int. J. Engng. Sci. 38, 1219–1234.

Ru, C.Q., 1999. Conducting cracks in a piezoelectric ceramic of limited electrical polarization. J. Mech. Phys. Solids 47, 2125–2146.

Suo, Z., 1993. Models for breakdown-resistant dielectric and ferroelectric ceramics. J. Mech. Phys. Solids 41, 1155–1176.

Wang, X., Zhong, Z., 2002. A conducting arc crack between a circular piezoelectric inclusion and an unbounded matrix. Int. J. Solids Struct. 39, 5895–5911.

Yoffe, E.H., 1951. The moving Griffith crack. Philos. Mag. 42, 739–750.